

## *Supplementary Material*

### **Dual inhibitory potential of ganoderic acid A on GLUT1/3: Computational and *in vitro* insights into targeting glucose metabolism in human lung cancer**

**Mona Alrasheed Bashir<sup>a,b,c</sup>, Mohnad Abdalla<sup>d,e</sup>, Chang-Sheng Shao<sup>a,b</sup>, Han Wang<sup>a,b</sup>, Precious Bondzie-Quaye, Waleed Abdelbagi Ahmed<sup>f</sup>, Mohammed Sharif<sup>a,b</sup>, Qing Huang<sup>a,b\*</sup>**

<sup>a</sup> CAS Key Laboratory of High Magnetic Field and Ion Beam Physical Biology, Institute of Intelligent Machines, Hefei Institutes of Physical Science, Chinese Academy of Sciences, Hefei, 230031, China

<sup>b</sup> Science Island Branch of Graduate School, University of Science and Technology of China, Hefei 230026, China

<sup>c</sup> Department of Biotechnology, Faculty of Science and Technology, Omdurman Islamic University, Omdurman, P.O. Box 382, Sudan

<sup>d</sup> Pediatric Research Institute, Children's Hospital Affiliated to Shandong University, Jinan, Shandong 250022, China

<sup>e</sup> Shandong Provincial Clinical Research Center for Children's Health and Disease, Jinan, Shandong 250022, China

<sup>f</sup> Anhui Province Key Laboratory of Medical Physics and Technology, Institute of Health and Medical Technology, Hefei Institutes of Physical Science, Chinese Academy of Sciences, Hefei, 230031, China

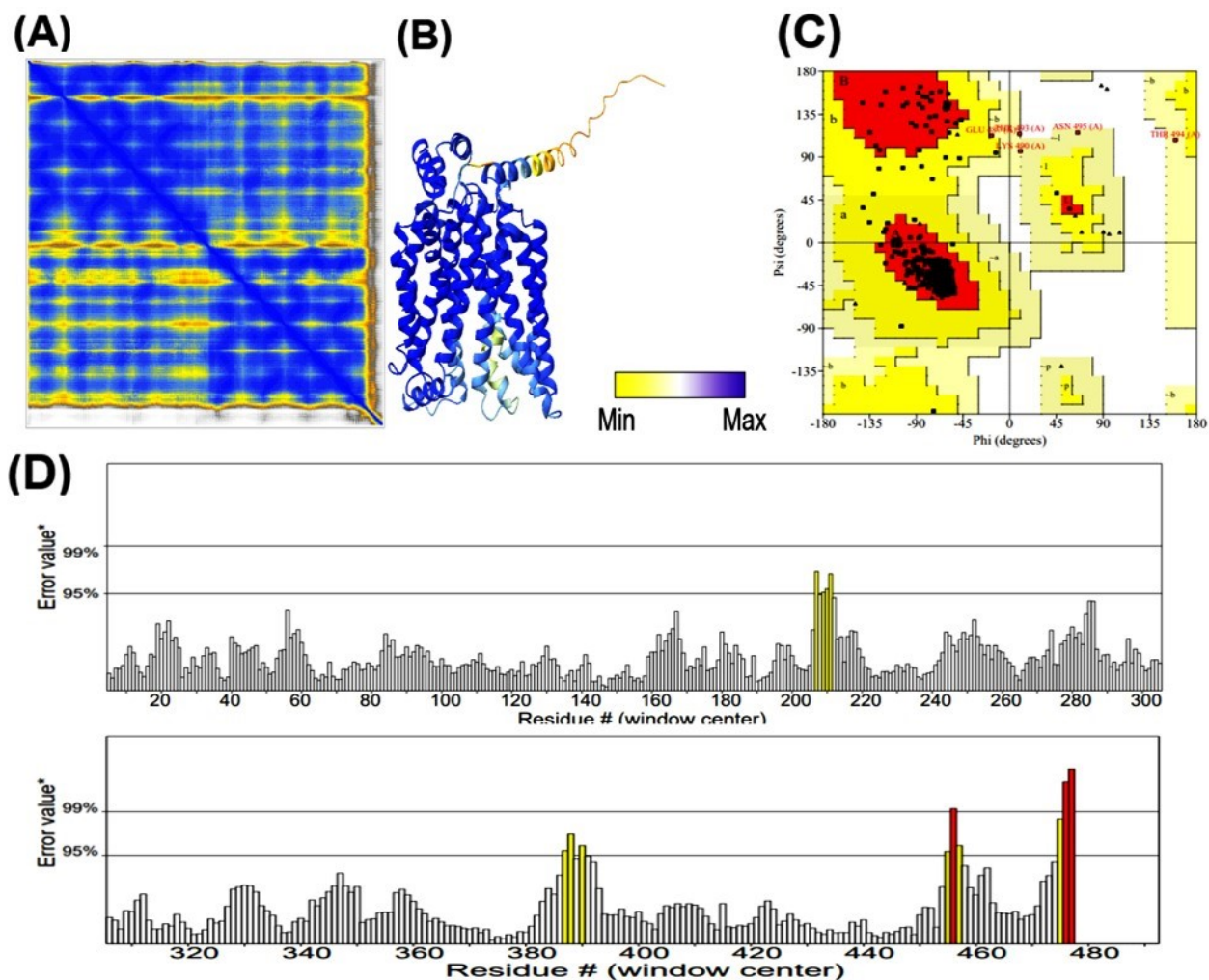


**Figure S1. Validation and quality evaluation of the predicted structure of GLUT3 in an in-ward open conformation (GLUT3endo) before energy minimization.** Plot (A&B) shows the Predicted Aligned Error (PAE) and predicted local distance difference test (pLDDT), the high-confident areas in the structure are in blue, whereas the areas with low confidence are in yellow. (C) displays Ramachandran plot (PROCHECK), while (D) represents ERRAT analysis as calculated by SAVES v6.0. ERRAT analysis displays the result as the percentage of the protein for which the calculated error values fall below the 95% rejected limit. Good high-resolution structures generally produce values around 95% or higher, while for lower resolutions (2.5 to 3Å) the average overall quality factor is around 91%.

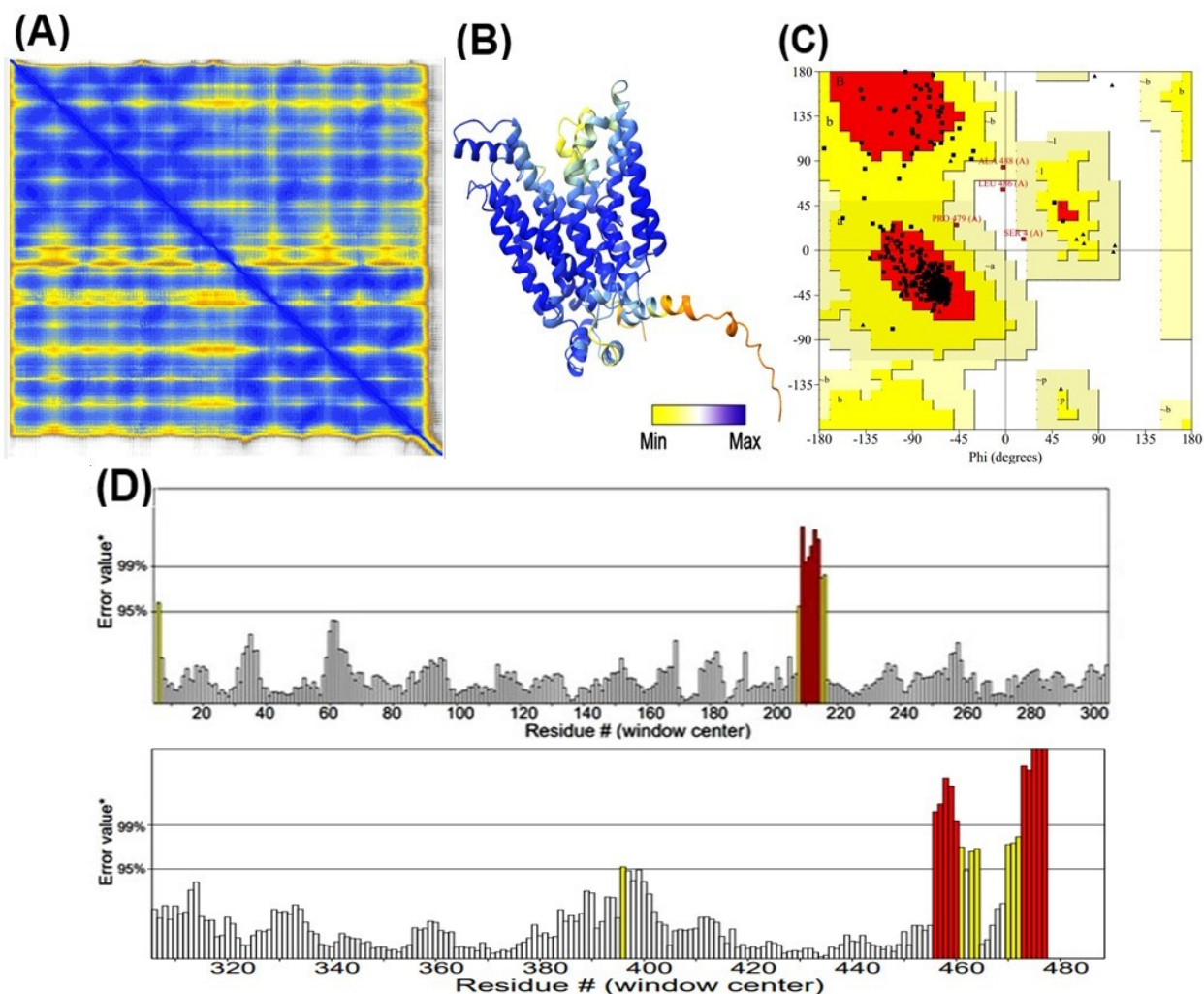


**Figure S2. Validation and quality evaluation of GLUT1exo in an outward open conformation (GLUT1exo) before energy minimization.** (A&B) show the Predicted Aligned Error (PAE) and predicted local distance difference test (pLDDT). The high Confidence areas in the structure are in blue, whereas the areas with low confidence are in yellow. (C) displays Ramachandran plot (PROCHECK), while (D) represents ERRAT analysis as calculated by SAVES v6.0. ERRAT analysis displays the result as the percentage of the protein for which the calculated error values fall below the 95% rejected limit. Good high-resolution structures generally produce values around 95% or higher, while for lower resolutions (2.5 to 3Å) the average overall quality factor is around 91%.

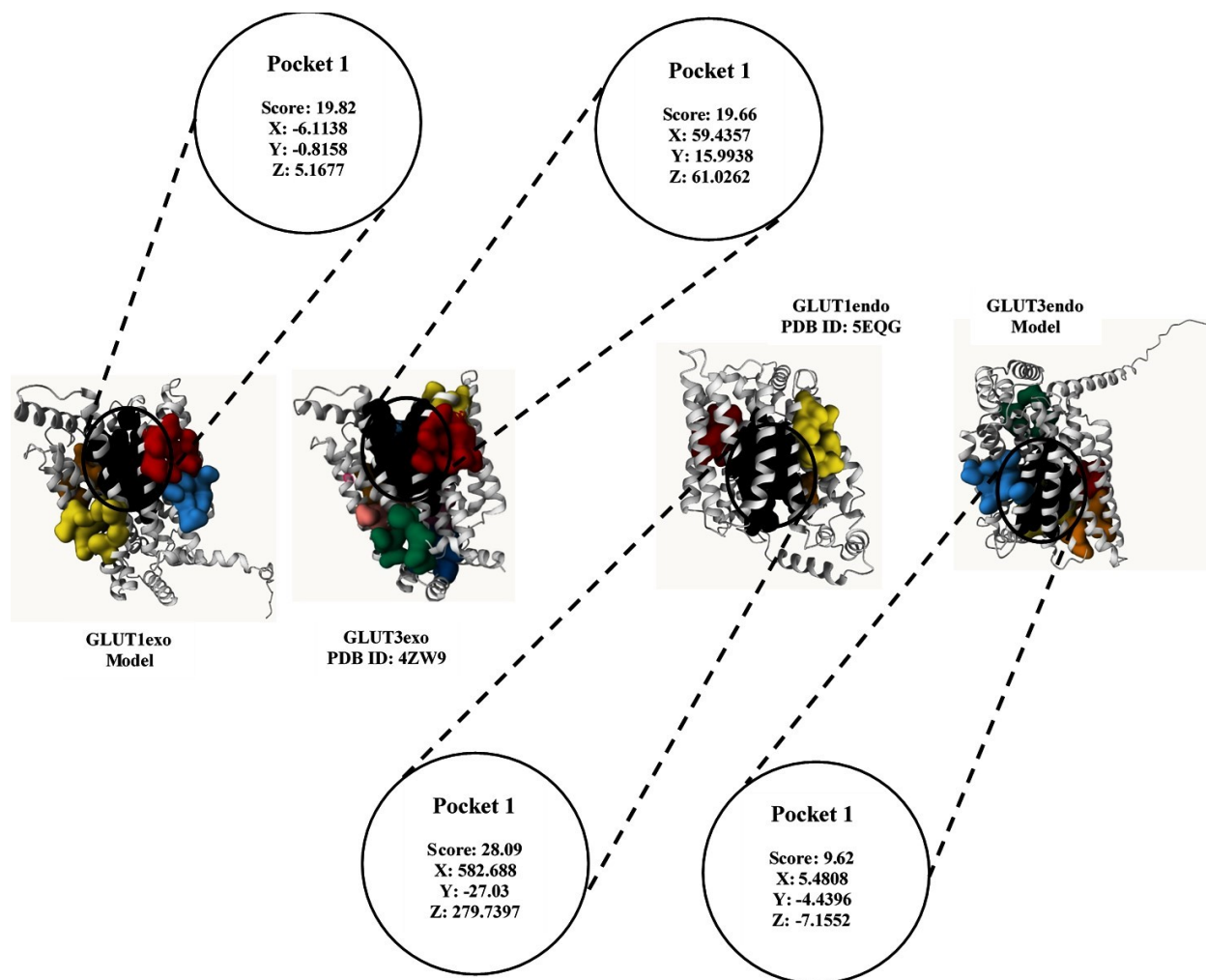


**Figure S3 shows the binding pockets of GLUT1 and GLUT3 proteins.** Surface with black, red, yellow, orange, blue, green, dark blue, purple, and peach colors representing the pockets; P1, P2, P3, P4, P5, P6, P7, P8, and P9, respectively with their pocket one's score and the grid box XYZ dimensions of the GLUT1 and GLUT3 proteins in endofacial and exofacial conformations.

**Supplementary Table 1: The putative binding pockets of GLUT1/3 rank, pocket volume, and residues.**

Protein	Pocket Rank	Volume (Å <sup>3</sup> )	Residues
<b>GLUT1exo Model</b>	1	2281.1	A_161, A_164, A_168, A_172, A_26, A_282, A_283, A_287, A_288, A_291, A_295, A_30, A_31, A_310, A_314, A_317, A_33, A_34, A_35, A_379, A_388, A_411, A_412, A_415, A_419, A_69, A_70, A_72, A_73
	2	292.8	A_284, A_417, A_418, A_421, A_422, A_425, A_436, A_437, A_440
	3	146.0	A_101, A_102, A_131, A_78, A_82, A_86, A_98, A_99
	4	222.1	A_170, A_174, A_192, A_195, A_196, A_24, A_28
	5	164.7	A_273, A_277, A_280, A_443, A_444, A_447
<b>GLUT1endo PDB ID: 5EQG</b>	1	2582.8	A_137 A_138 A_141 A_142 A_160 A_161 A_164 A_165 A_168 A_26 A_282 A_283 A_287 A_288 A_291 A_292 A_30 A_317 A_379 A_380 A_384 A_385 A_388 A_392 A_401 A_404 A_405 A_408 A_411 A_412 A_415 A_80 A_83
	2	276.7	A_284 A_417 A_418 A_421 A_422 A_425 A_436 A_437 A_440
	3	300.6	A_170 A_174 A_192 A_196 A_21 A_24 A_25 A_28
	4	77.1	A_102 A_131 A_78 A_82 A_86 A_99
<b>GLUT3exo PDB ID: 4ZW9</b>	1	2414.6	A_159, A_162, A_166, A_24, A_28, A_280, A_281, A_285, A_286, A_287, A_290, A_291, A_294, A_315, A_32, A_35, A_377, A_378, A_386, A_409, A_410, A_413, A_414, A_417, A_418, A_421, A_60, A_63, A_64, A_67, A_68, A_70, A_71
	2	351.4	A_282, A_415, A_416, A_419, A_420, A_423, A_431, A_434, A_435, A_438
	3	452.3	A_291, A_295, A_298, A_353, A_420, A_424, A_428, A_429, A_431, A_432
	4	376.7	A_15, A_161, A_164, A_168, A_18, A_19, A_190, A_194, A_197, A_22
	5	247.9	A_166, A_170, A_28, A_286, A_289, A_29, A_290, A_308, A_32
	6	260.1	A_255, A_256, A_257, A_400, A_403, A_79, A_82, A_83, A_86
	7	98.6	A_146, A_148, A_210, A_230, A_238, A_241, A_458
	8	109.9	A_150, A_153, A_154, A_323, A_6
	9	39.2	A_134 A_198 A_94 A_97
<b>GLUT3endo Model</b>	1	1019.9	A_159 A_162 A_166 A_170 A_24 A_28 A_281 A_285 A_286 A_289 A_29 A_290 A_308 A_315 A_32 A_377 A_378 A_386 A_409 A_413
	2	312.2	A_282 A_416 A_419 A_420 A_423 A_431 A_434 A_435 A_438
	3	1325.3	A_27 A_28 A_286 A_287 A_290 A_291 A_31 A_35 A_413 A_414 A_417 A_418 A_421 A_63 A_64 A_67 A_68 A_70 A_71
	4	397.2	A_291 A_294 A_295 A_298 A_353 A_420 A_424 A_428 A_429 A_432
	5	234.8	A_164 A_18 A_19 A_190 A_194 A_197 A_22
	6	321.1	A_254 A_255 A_257 A_400 A_403 A_79 A_82 A_83 A_86

**Supplementary table 2. The interacted amino acids around GAA, CCB, and PHT in GLUT1/3 complexes in endo- and exofacial conformations.**

No.	Ligand-protein complex	Hydrogen bonding	Hydrophobic interactions
1	<b>GAA-GLUT1endo</b>	ASN288, HIS160	PRO141, GLN161, ILE164, VAL165, PHE291, ILE287, TRP388
2	<b>GAA-GLUT3endo</b>	GLN281, TYR291, ASN413	TYR290, TYR291, ASN413, ASN286, VAL67, THR28, PHE24
3	<b>CCB- GLUT1endo</b>	THR137, PRO385	PHE26, GLN161, ILE164, VAL165, THR321, PRO385, TRP388, TRP412
4	<b>CCB- GLUT3endo</b>	THR28, GLN281, ASN286, TYR386	PHE24, ILE161, ILE166, ASN286, TYR290, PHE377, TRP386, TRP410
5	<b>GAA-GLUT1exo</b>	GLN283, ASN288, ASN317, ASN415	THR30, ASN288, TYR292, GLN423
6	<b>GAA-GLUT3exo</b>	THR28, GLN281, TYR291, ASN413	THR28, TYR290, TYR291, ASN413
7	<b>PHT- GLUT1exo</b>	GLN161, GLN172, GLN282, GLN283, TRP388, ASN415	ILE164, ILE168, GLN282, <b>PHE291*</b> , PHE379,
8	<b>PHT- GLUT3exo</b>	TYR291, ASN413	VAL67, ASN286, TYR290, TYR291, PRO421

\*This residue formed  $\pi$ -stacking with Phloretin in the PHT-GLUT1exo complex.



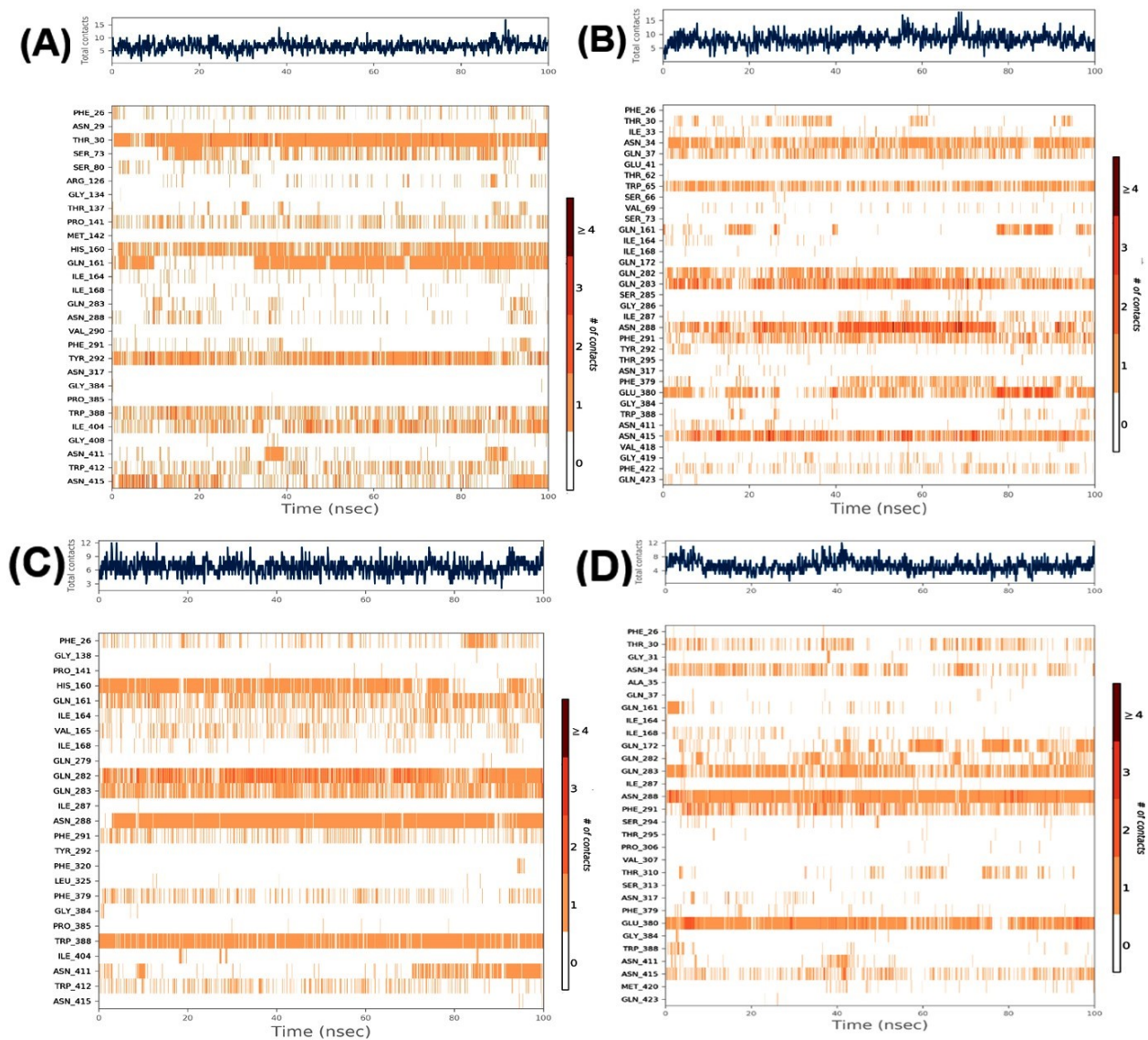
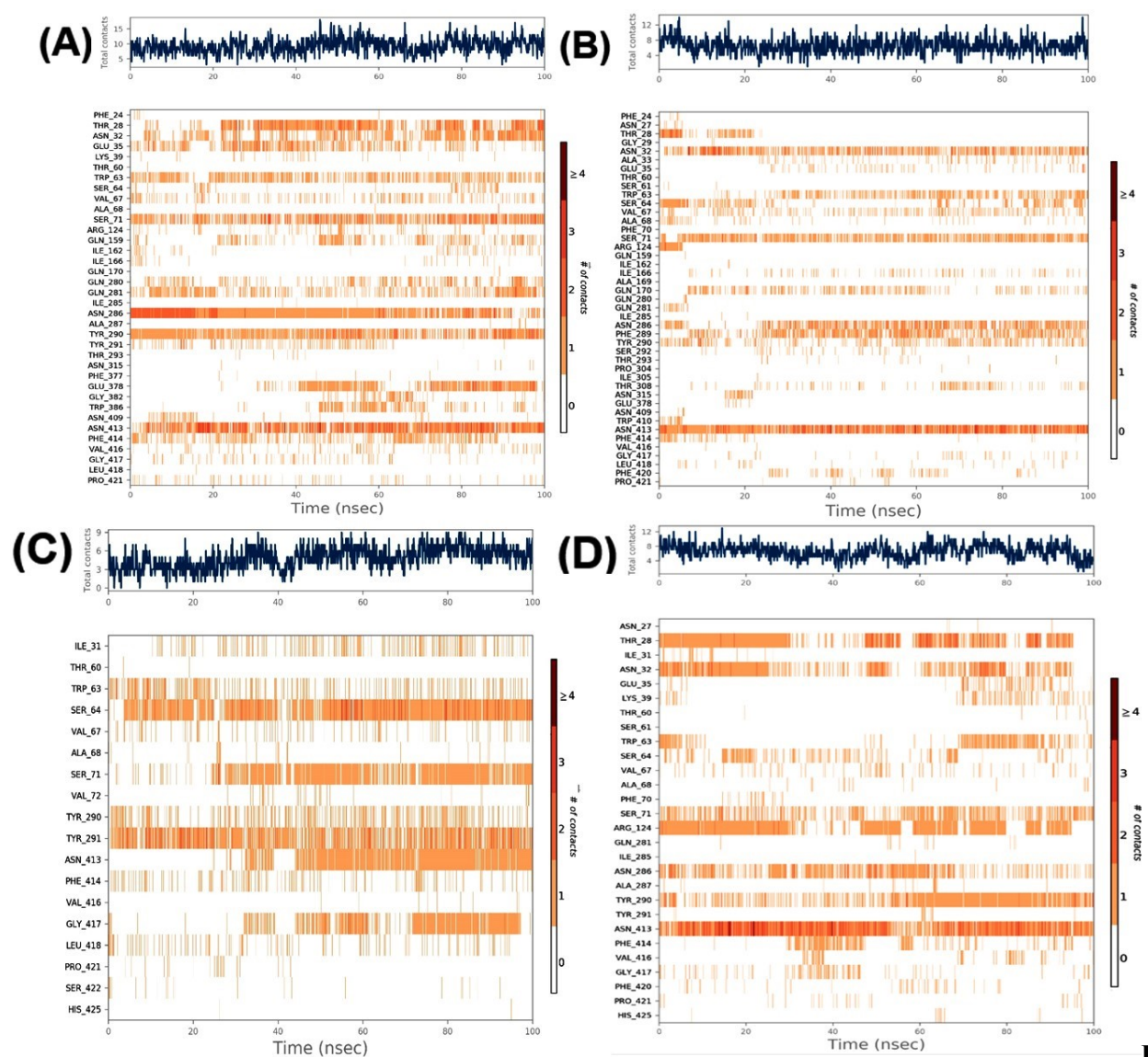


**Figure S4** shows the protein-ligand contact map of GLUT1 during 100 ns. Plots (A&B) display the residues in contact with GAA in endo- and exofacial conformation, respectively. While (C&D) plots show the residues in contact with Cytochalasin B and Phloretin, respectively.



**F** figure S5 shows the protein-ligand contact map of GLUT3 during 100 ns. Plots (A&B) display the residues in contact with GAA in endo- and exofacial conformation, respectively. While (C&D) plots show the residues in contact with Cytochalasin B and Phloretin, respectively.



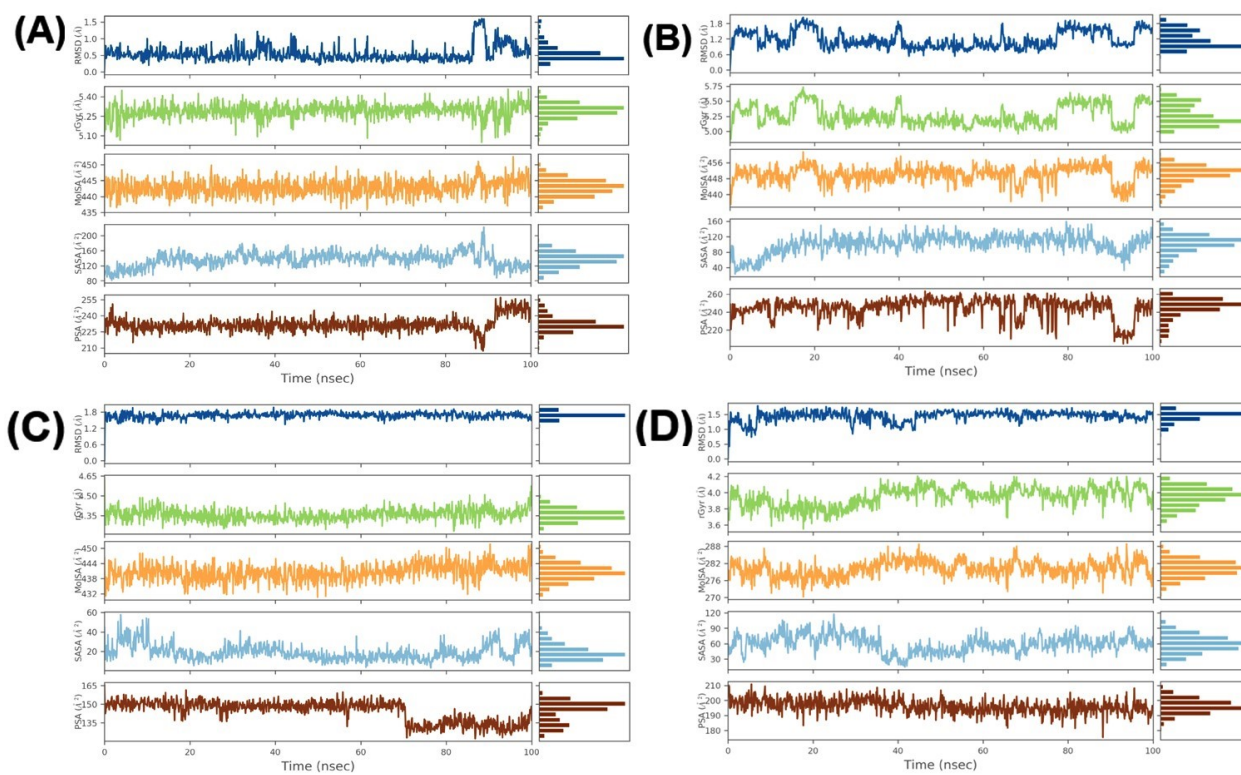


**Figure S6** shows the ligand's properties within GLUT1 during 100 ns. Plots (A&B) display GAA in endo- and exofacial conformation, respectively. While (C&D) plots show Cytochalasin B and Phloretin with GLUT1, respectively.

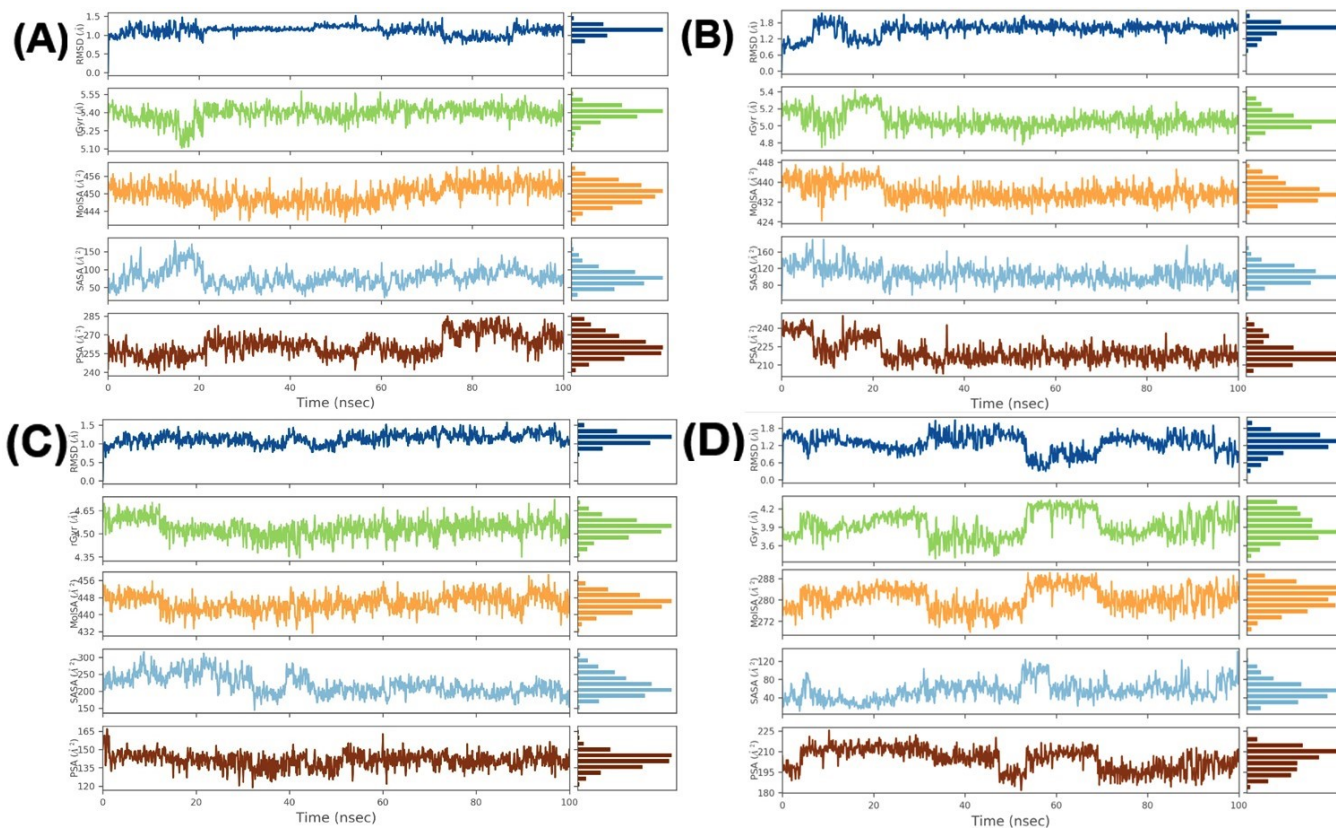


**Figure S7** shows the ligand's properties within GLUT3 during 100 ns. Plots (A&B) display GAA in endo- and exofacial conformation, respectively. While (C&D) plots show the Cytochalasin B and Phloretin with GLUT3, respectively.

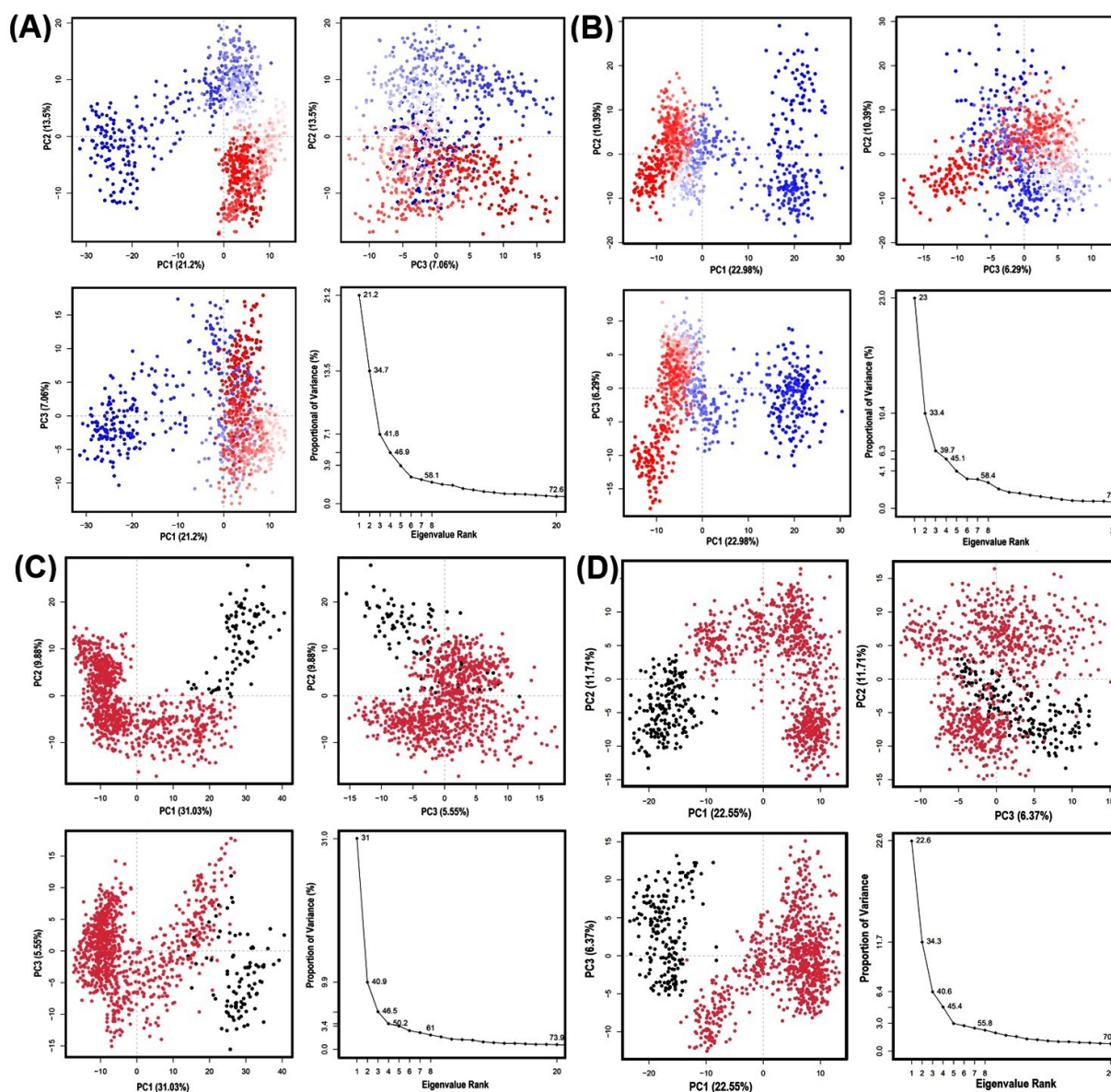


**Figure S8. PCA of top three Principal component analysis of 100 ns, along with eigenvalue rank plots. (A-D) Plots represent CCB-GLUT1endo, Phlo-GLUT1exo, CCB-GLUT3endo, and Phlo-GLUT3exo, respectively. The plot had multiple data points, where each one denoting the conformation of the protein. A color gradient indicates the initial to final stages of the simulation (blue to red for GLUT1 and red to black for GLUT3).**

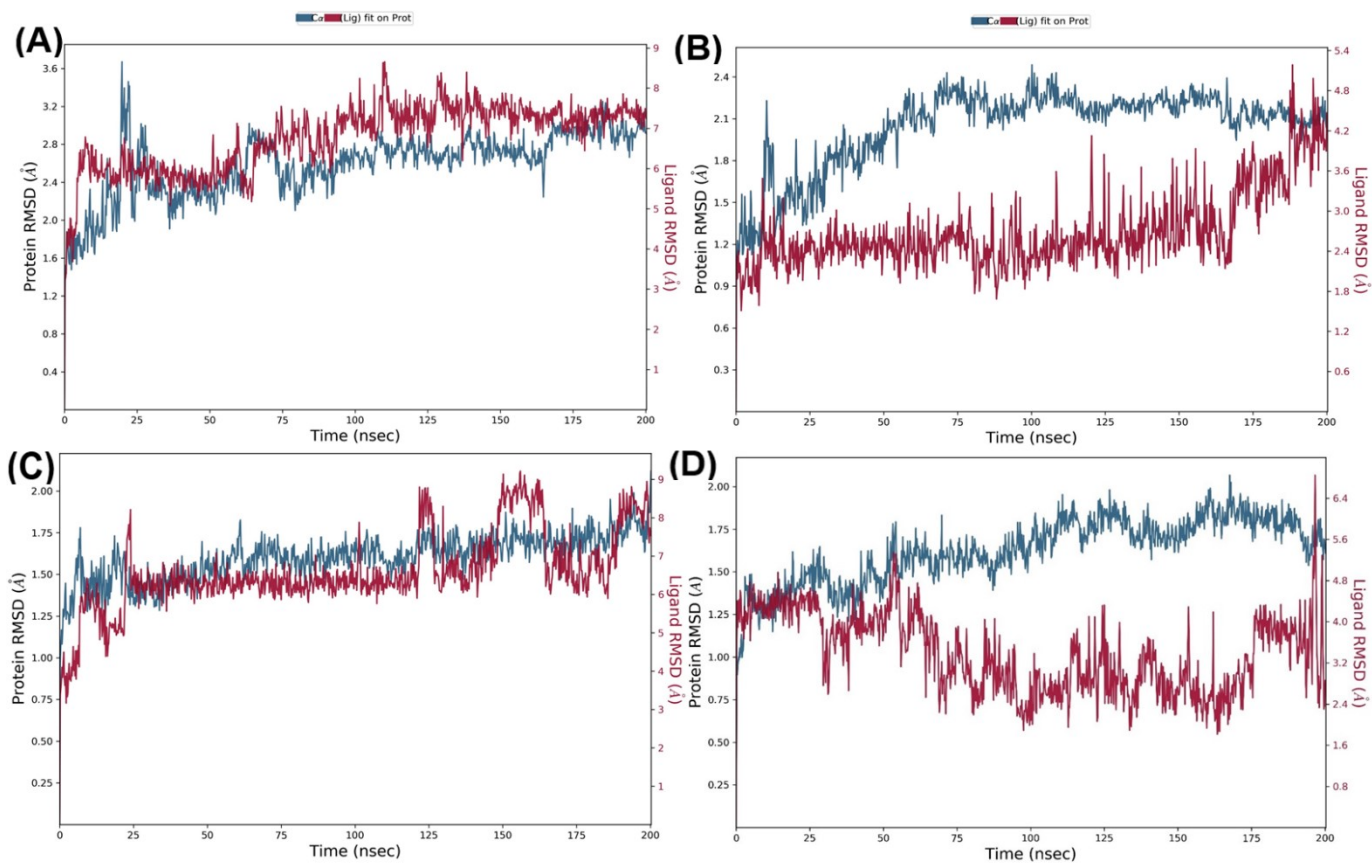


**Figure S9. RMSD study plots of ligand-GLUT3 complexes over 200 ns.** (A and B) represent the RMSD plots for the GLUT3endo-GAA and GLUT3endo-CCB, respectively. While (C and D) for the GLUT3exo-GAA and GLUT3exo-phlo, respectively.



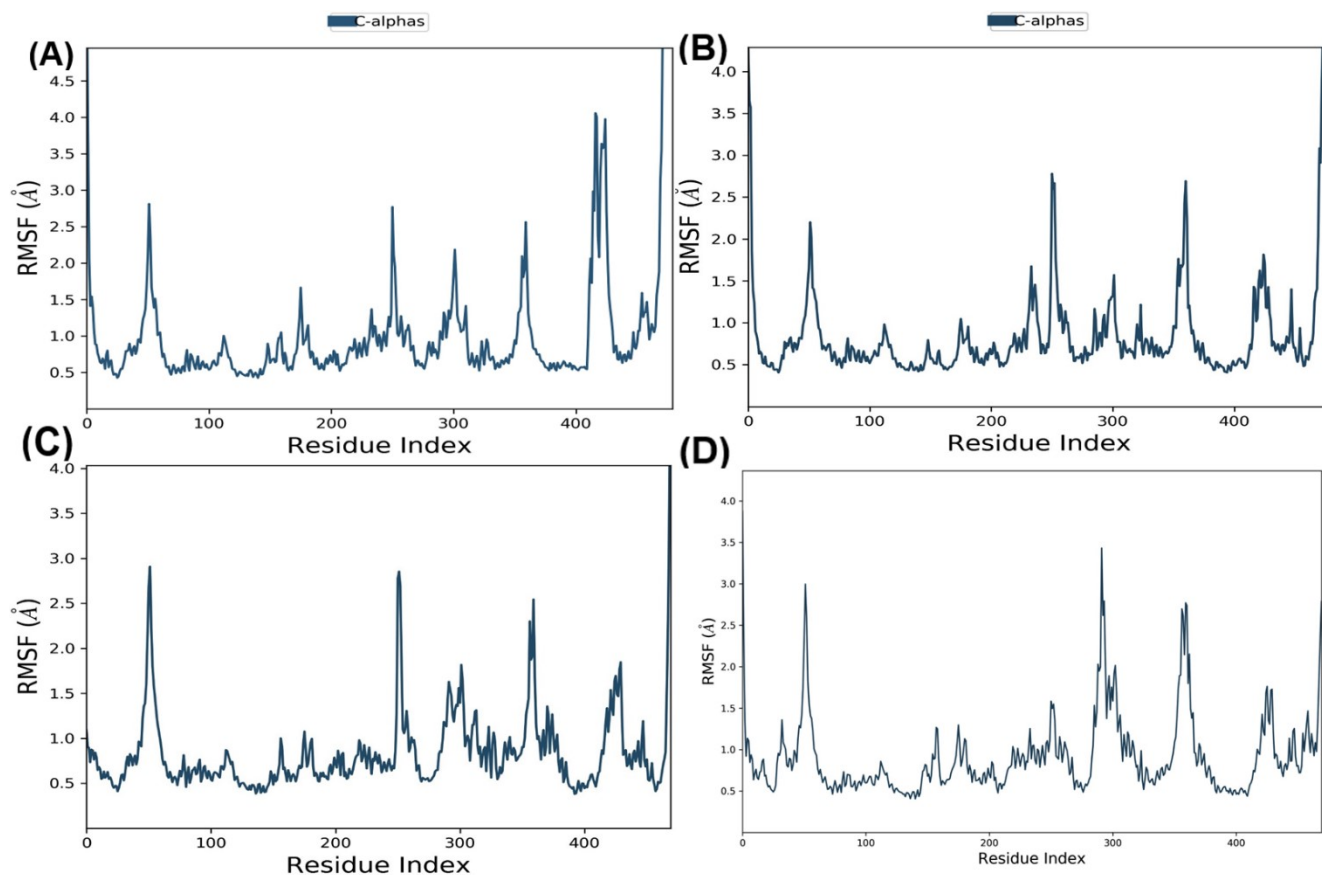


**Figure S10. RMSF study plots of ligand-GLUT3 complexes. during 200 ns.** (A&B) represent the RMSF plots for the GLUT3endo-GAA and GLUT3endo-CCB, respectively. While (C&D) for the GLUT3exo-GAA and GLUT3exo-phlo, respectively.



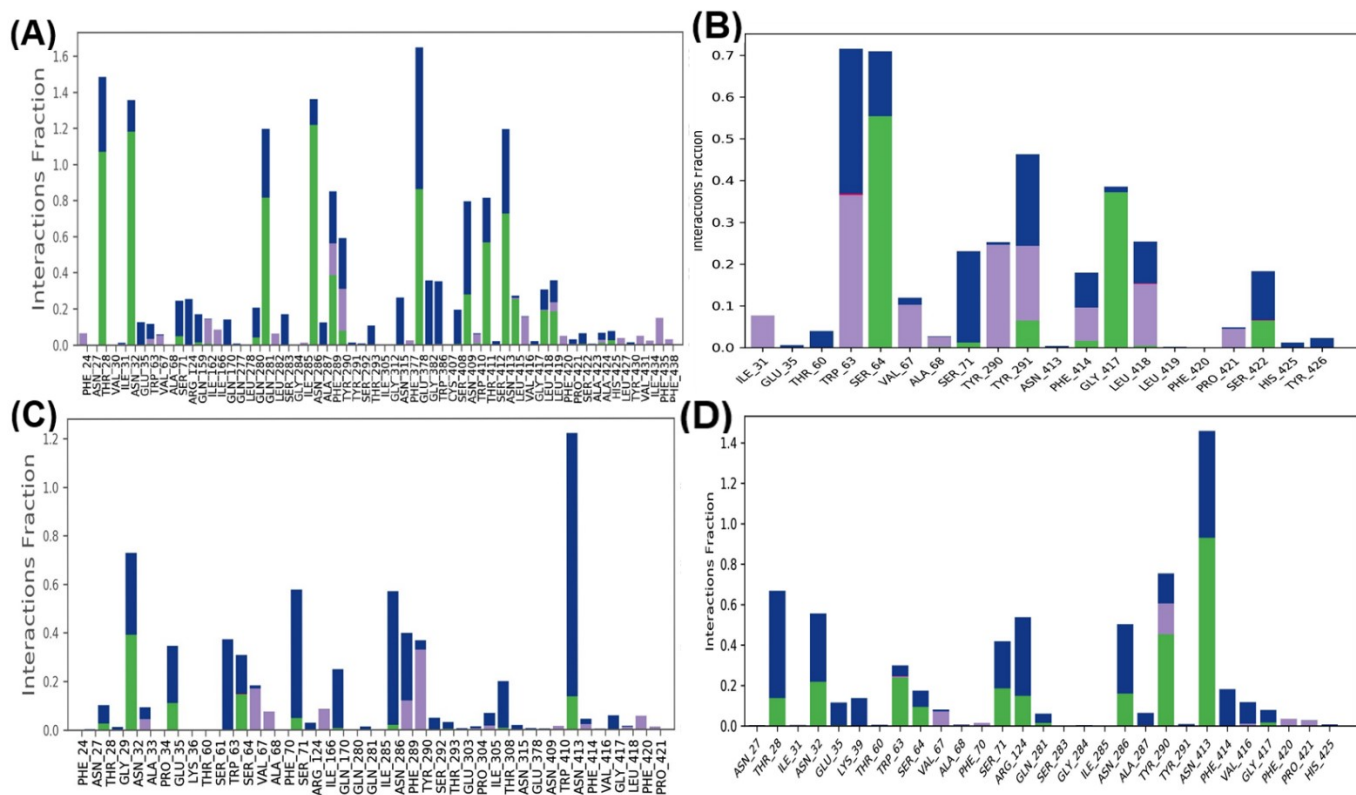


**Figure S11. The histogram of GLUT3-ligand interaction during 200 ns.** (A-D) Plots represent GAA-GLUT3endo, CCB-GLUT3endo, GAA-GLUT3exo, and Phlo-GLUT3exo, respectively. The histogram of protein-ligand interaction displays hydrogen bonding in green color, water bridges in blue, and hydrophobic bonds in violet.

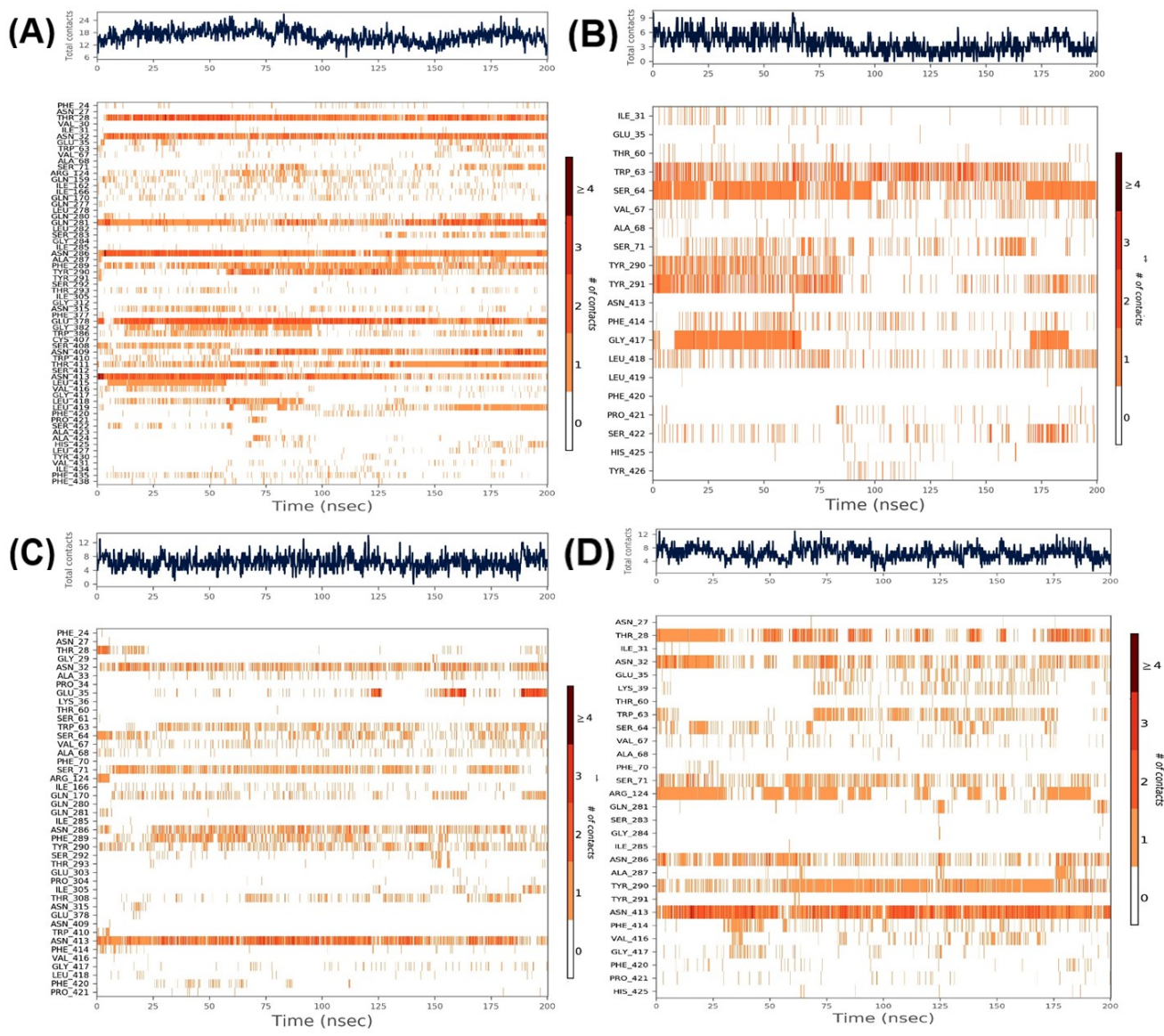


**Figure S12** shows the protein-ligand contact map of GLUT3 during 200 ns. Plots (A&B) display the residues of GLUT3 in contact with GAA and Cytochalasin B in endofacial conformation, respectively. While (C&D) plots show the residues in contact with GAA and Phloretin in exofacial conformation, respectively.

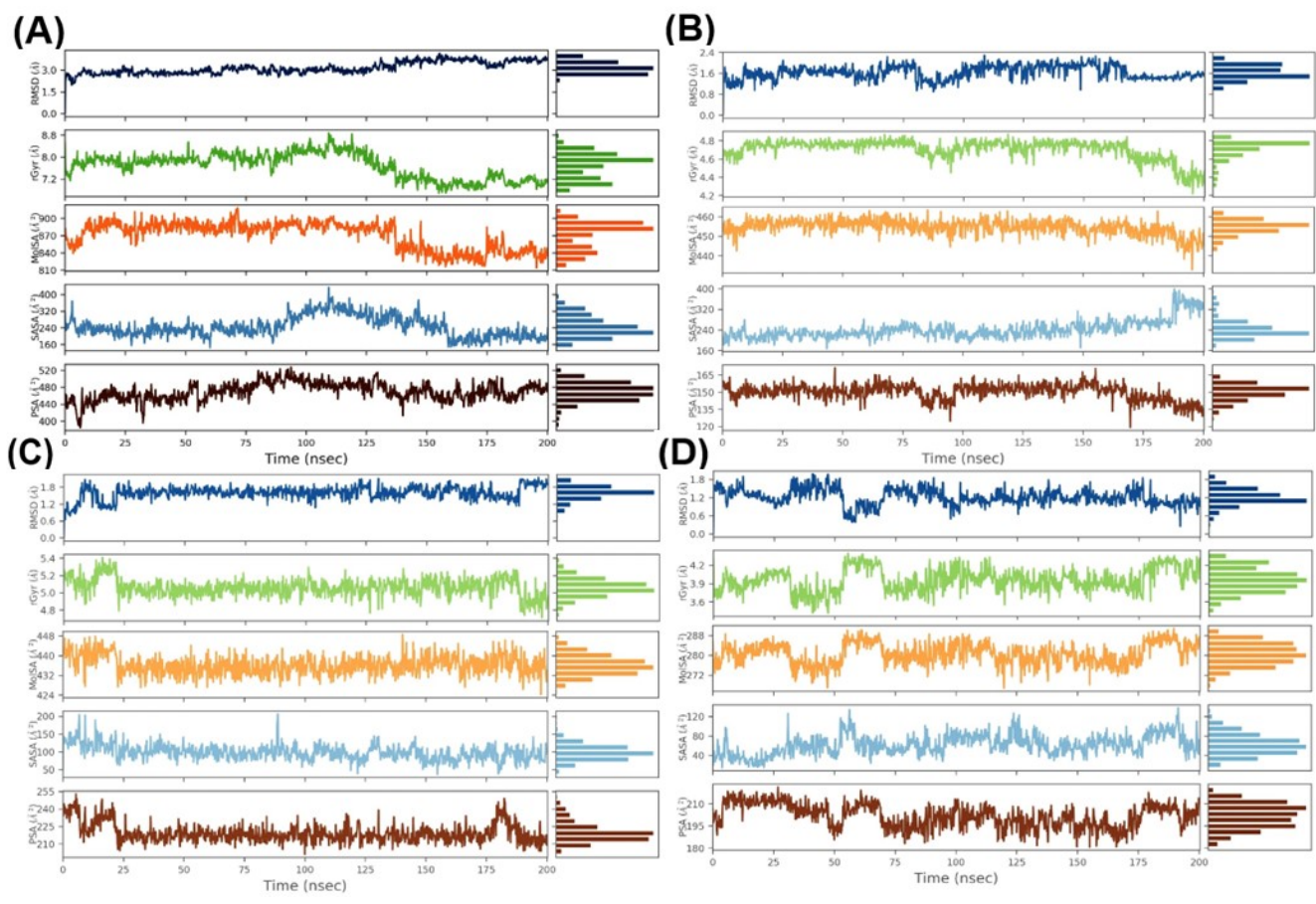


**Figure S13** shows the ligand's properties within GLUT3 during 200 ns. Plots (A&C) display GAA in endo- and exofacial conformation, respectively. While (C&D) plots show the Cytochalasin B and Phloretin with GLUT3, respectively



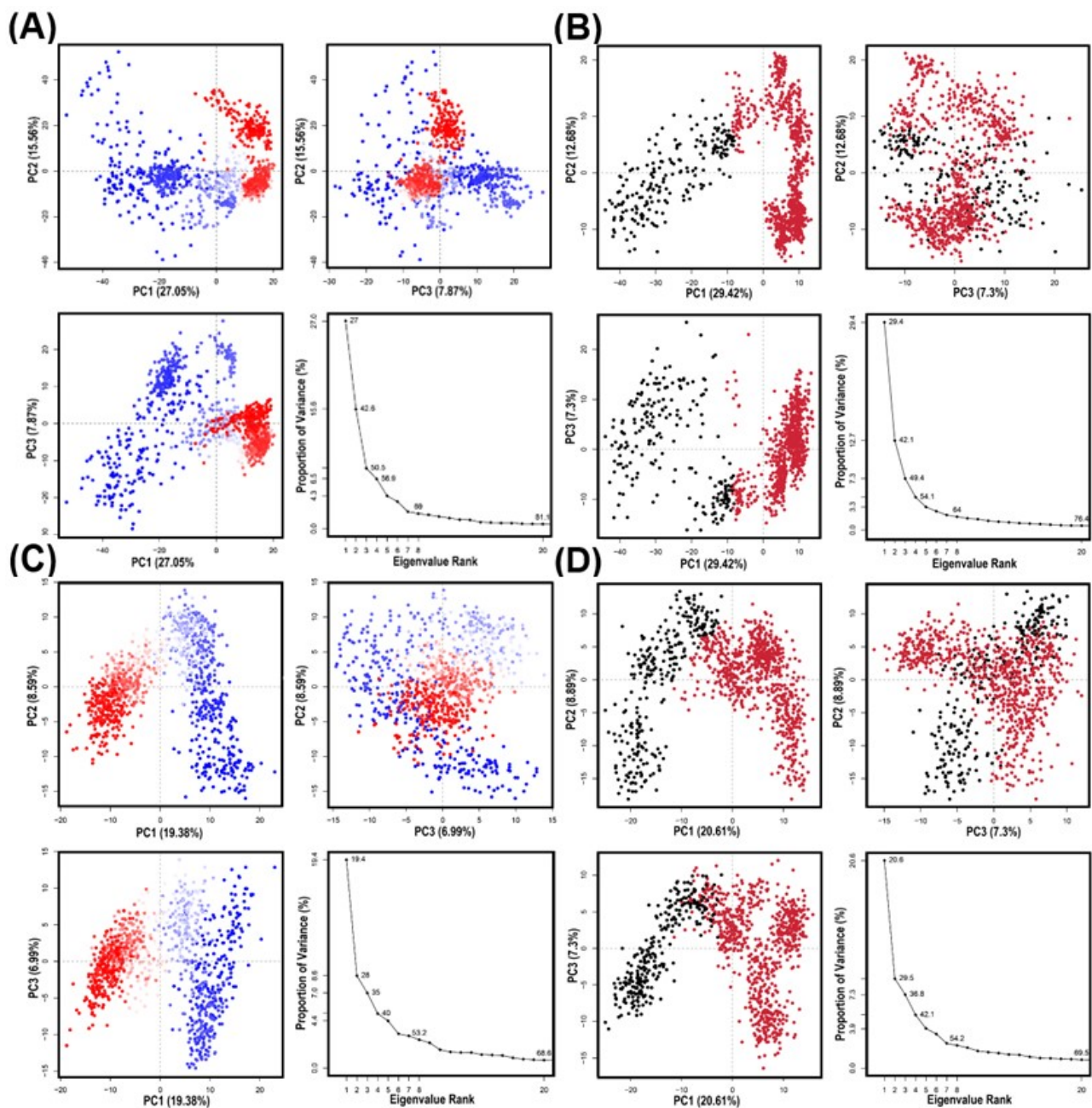


**Figure S14. PCA of top three Principal component analysis of 200 ns, along with eigenvalue rank plots. (A-D) Plots represent GLUT3endo-GAA, GLUT3endo-CCB, GLUT3exo-GAA, and GLUT3exo-phlo, respectively. The plot had multiple data points, where each one denoting the conformation of the protein.**

Supplementary Table 3 shows the primer sequences of qRT-PCR reactions.

No.	Target	Sequence
1	<b>GLUT1</b>	Forward: GCCTGAAGTCGCACAGTGAATAA
		Reverse: GCTCATTGGGCCCATACAAAG
2	<b>GLUT3</b>	Forward: CAAGTCACAGTGCTAGAGTCTTTC
		Reverse: GGAGAGCTGGAGCATGATAGAGAT
3	<b><math>\beta</math>-actin</b>	Forward: GTCTCCTCTGACTTCAACAGCG
		Reverse: ACCACCCTGTTGCTGTAGCCAA

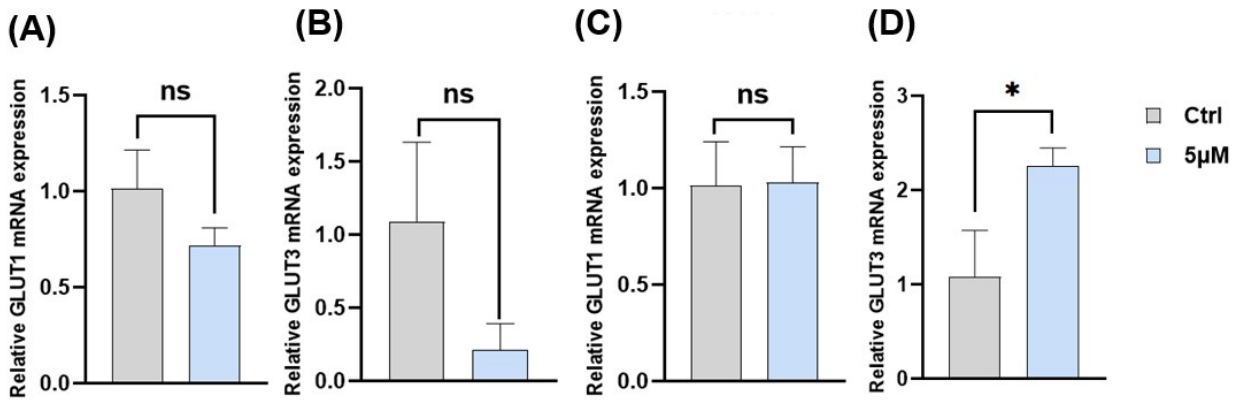


Figure S15 shows the effect of GAA on GLUT1/3 gene expression in human lung cancer cell lines. Plots (A&B) and (C&D) display the effect of GAA on GLUT1 and GLUT3 in A549 and H1299, respectively. Statistical significance is denoted as follows: \*P < 0.05; \*\*P < 0.01; \*\*\*P < 0.001.

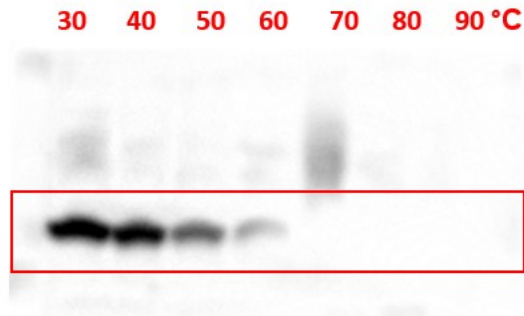


**Western blot results:**

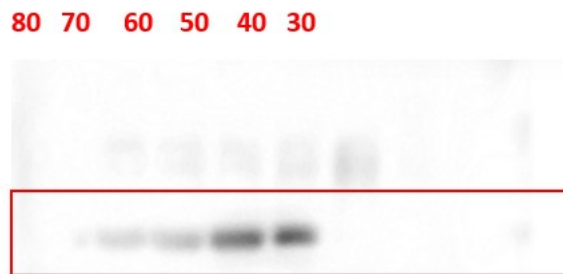
**1- A549 cell lines**

**1.2 Western blot result of cellular thermal shift assay**

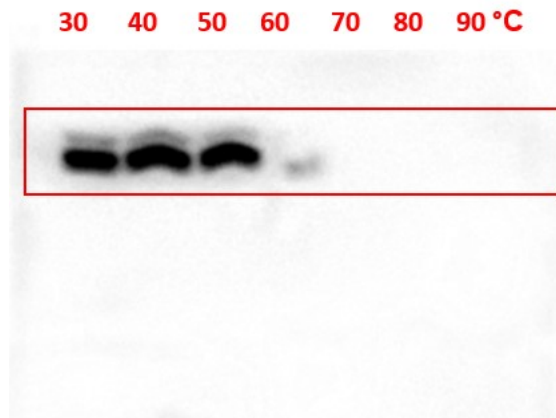
**1.2.1. GLUT1-GAA**



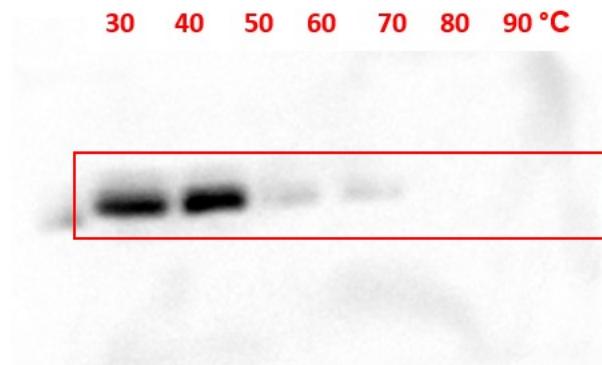
**1.2.1. GLUT1-DMSO**



**1.2.3. GLUT3-GAA**



### 1.2.3. GLUT3-DMSO



## 2- H1299 cell lines

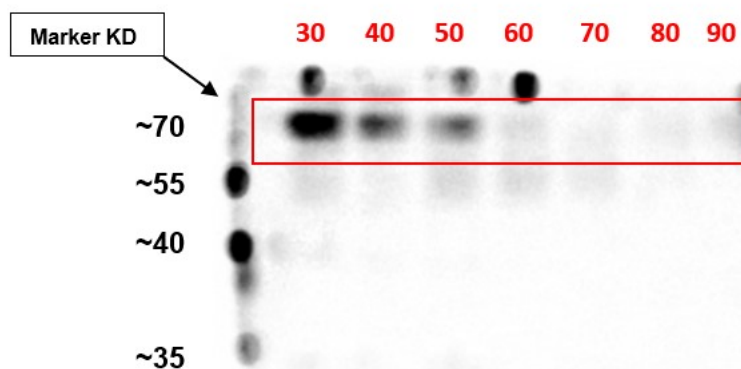
**Note:** These cell lines expressed GLUT1/3 in glycosylated proteins in which the molecular weight reaches 70KD instead of 55 KD as reported earlier”

### 2.1 Western blot result of cellular thermal shift assay

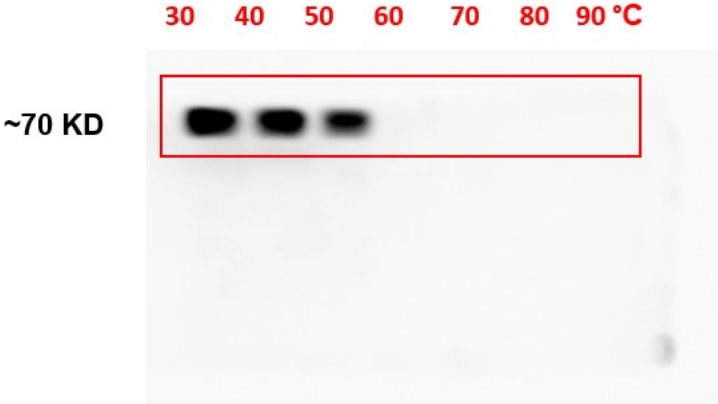
#### 2.1.1 GLUT1-GAA



#### 2.1.2 GLUT1-DMSO



**2.1.3 GLUT3-GAA**



**2.1.4 GLUT3-DMSO**

